**American Journal of Engineering Research (AJER)**
e-ISSN: 2320-0847 p-ISSN : 2320-0936
Volume-4, Issue-6, pp-18-30
www.ajer.org
Research Paper Open Access

# Measurement and Analysis of Magnetic Barkhausen Noise on the Surface of Grain Oriented Electrical Steels at Power Frequency.

Nkwachukwu Chukwuchekwa[1], Onojo J. Ondoma[1] and Joy U. Chukwuchekwa[2]
[1]*Electrical/Electronic Engineering Department, Federal University of Technology Owerri, Nigeria*
[2]*Department of Mathematics, Federal University of Technology Owerri Nigeria*

***ABSTRACT:*** *Magnetic characteristics of Grain-Oriented Electrical Steel are generally measured at high flux densities (above 0.2 T) for applications in all electromagnetic devices. However, magnetic measurements at very low inductions are useful for characterisation of electrical steel used as cores of metering current transformers and low frequency magnetic shielding such as for protection from high field magnetic resonance imaging (MRI) medical scanners. In this work, Barkhausen noise, which is a non-destructive evaluation means of characterisation of electrical steels was accurately measured at very low flux densities for several samples of Conventional grain-oriented (CGO) and High Permeability grain-oriented (HGO) electrical steels. High flux density measurements were also carried out and compared. The results show that the Barkhausen signal amplitude sum and the root mean square values are higher for HGO than CGO steels at high flux densities. However, at lower flux densities the trend reverses. HGO steels are adjudged to have better magnetic properties than CGOs and so are more expensive but this work shows that CGO steels are better for very low flux density applications. This new understanding of low flux density performance of engineering magnetic materials will provide manufacturers with a more reliable and meaningful foundation for their designs.*

***KEY WORDS*****:** *Amplitude sum, Barkhausen noise, Electrical steel, RMS, Grain size*

## I. INTRODUCTION

Electrical steel is comprised of grain oriented and non-grain oriented steels. Grain oriented electrical steel (GOES) is so called because it contains a grain structure with a distinct preferred orientation. The relative permeability and power loss are optimised when the material is magnetised along this direction of preferred orientation. For this reason GOES is usually used in the construction of medium to large transformer cores. GOES is comprised of the conventional grain oriented (CGO) and high permeability grain oriented (HGO) steels.

Non grain oriented (NGO) electrical steels contain a much finer grain structure and exhibit little or no preferred orientation. They are most commonly used in applications such as rotating electrical machines and small transformers used in domestic appliances that require isotropic magnetic properties in the plane of the sheet. In these applications, the magnetic flux is oriented at various angles with respect to the rolling direction of the sheet. As these materials are extensively used, they are responsible for a large portion of the energy loss in electrical power systems because of the non-linearity of the B-H characteristic. For this reason, the study and the control of the magnetic and microstructural parameters of these steels becomes a very important economic issue [1] and this accounts for the reason why these materials are investigated in this study.

Barkhausen Noise (BN) is a very important tool for non-destructive characterisation [2-4]. The BN mechanism can provide understanding of the microstructure of the material, without the use of laborious methods such as the Epstein frame typically used for characterisation of electrical steels. The Barkhausen effect arises from the discontinuous changes in magnetisation under the action of a continuously changing magnetic field when domain walls encounter pinning sites [5]. This noise phenomenon can be investigated statistically through the detection of the random voltage observed on a search coil placed on the surface or encircling the material during the magnetisation of the material. BN are related to the way domain walls interact with pinning sites, such as defects, precipitates and grain boundaries, as domains reorganise to align magnetic moments in the direction of the applied magnetic field. The number of Barkhausen emissions is determined by the number of pinning sites provided that the volume of the sites is sufficient to cause pinning. BN is therefore an important tool for evaluating the scale of interaction between pinning sites of varying sizes and magnetic domains [6].

Microstructural features such as grain size, number and distribution of pinning sites, grain boundaries and grain-grain misorientation are the main parameters that distinguish CGO from HGO steels in relation to their bulk magnetic properties. Magnetic characteristics of electrical steel are usually measured at the high flux densities suitable for applications in power transformers, motors, generators, alternators and a variety of other electromagnetic applications. Magnetic measurements at very low inductions are useful for magnetic characterisation of electrical steel used as cores of metering instrument transformers and low frequency magnetic shielding such as for protection from high field MRI (magnetic resonance imaging) medical scanners. Magnetisation levels in these applications are generally believed to be in the low flux density region so material selection based on high flux density grading is seriously flawed.

In this work, Barkhausen noise measurement was carried out on samples of CGO and HGO steels, 305 mm x 30 mm x 0.27 mm from two different producers named P1 and P2. 40 strips from P1 comprising 20 CGO and 20 HGO strips were tested. Another 40 strips from P2 comprising 20 CGO and 20 HGO strips were also tested. The average grain size for CGO is 4 mm and that of HGO is 9 mm. The samples were demagnetized by annealing in vacuum at 810° for 1 hour.

Each strip was singly magnetised under sinusoidal flux density, Bpeak, from 8.0 mT to 1.5 T at a magnetising frequency of 50 Hz. Each measurement of BN was made three times and then averaged. BN studies aimed at non-destructive testing applications are usually carried out under quasi-static or very low frequency magnetisation conditions but 50 Hz has been chosen in this work because it is believed that at this frequency the BN signal is possibly more related to dynamic processes and can give more information about the magnetisation processes which low frequency BN measurements cannot. Such information include eddy current anomalous loss influence on magnetisation.

## II. METHODOLOGY

A computer-controlled system capable of providing high accuracy and automatic measurements was developed for the measurement of BN of electrical steels at high and low flux densities. Figure 1 shows a schematic diagram of the system. It comprises a personal computer (PC) in which LabVIEW (Laboratory Virtual Instruments Engineering Workbench) version 8.5 from National Instruments (NI) was installed, a NI 4461 data acquisition (DAQ) card [7], an impedance matching transformer, Krohn-Hite model MT- 56R, to match the 600 Ω minimum load impedance of the DAQ card with the 5 to 20 Ω low impedance of the magnetising circuit, and a 4.7 Ω shunt resistor ($R_{sh}$) from Tyco Electronics BDS2A1004R7K having less than 40 nH inductance corresponding to reactance of 12.6 μΩ, so adds virtually no error to amplitude and phase of the current measurement. The shunt resistor has 100 W power rating and low Temperature Coefficient of Resistance (TCR) (150ppm/°C). Low TCR was necessary to ensure that changes in its temperature will not affect the overall accuracy of the system. The shunt was attached to a thermo electric heat sink device, model TDEX3132/100, in conjunction with silicon based thermal grease. A double vertical yoke made of grain-oriented (GO) steel which is 290 mm long and 32 mm wide was used. A 500-turn secondary winding (search coil, $N_2$), about 80 mm in length, was wound around a plastic former, 270 mm x 40 mm, housing the sample, while a 100-turn primary winding (magnetising coil), covering the entire length of the plastic former was wound over the secondary winding. A standard Epstein strip (305 mm x 30 mm) to be tested is placed between the yokes.

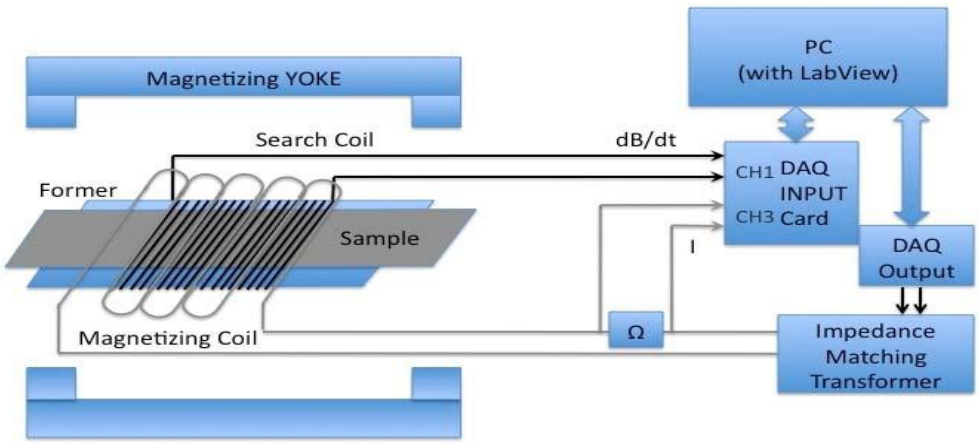


Fig 1: Block diagram of Barkhausen Noise measurement system.

The magnetising voltage was generated by the LabVIEW program through a voltage output from the DAQ card. The voltage drop across the shunt resistor, $V_{sh}$, and the secondary voltage, $e$ , were acquired by the

card for calculation of magnetic field strength and flux density respectively. The sampled waveforms of $e$ and $V_{sh}$ had 3000 points per cycle which is large enough to avoid quantization errors.
The instantaneous magnetic field strength, H (t) was calculated inside the LabVIEW program thus;

$$H(t) = \frac{N_1 i(t)}{l_m} \quad (1)$$

where $i(t) = \frac{V_{sh}}{R_{sh}}$, $N_1$ is the number of primary turns, $l_m$ is the magnetic path length, which is the distance between the inner edges of the yoke which is 0.27 m in this system.
The instantaneous flux density B (t) was obtained by means of digital integration of the $e$ signal as:

$$B(t) = -\frac{l\rho}{N_2 m}\int e dt \quad (2)$$

where $l$ is the sample length, m is the mass of the sample, and $\rho$ is the density of the sample. A feedback control system implemented in LabVIEW was used to control the flux density and to make the induced secondary voltage waveforms sinusoidal to have repeatable and comparable measurements. The form factor (FF) of the induced secondary voltage was maintained at $1.111 \pm 0.3\%$ which satisfies the recommendation in [8] to ensure that the time variation of the flux density was sinusoidal over the measurement range. Figure 2 shows the procedure for each measurement. Firstly, a table of peak flux density ($B_{peak}$) values and the measurement criteria which are the 0.3% error of $B_{peak}$ and the 0.3% error of the ideal FF of the induced secondary voltage was read. This is followed by applying the first magnetising waveform to the single sheet tester. If the criteria are met, the flux density and the magnetic field waveforms are averaged to minimise random errors and improve repeatability [9], otherwise the magnetising waveform is adjusted by the feedback algorithm. After averaging, the criteria are re-checked then the measurement data for this point is saved. A spread sheet file is generated if all the values of $B_{peak}$ are measured and the sample is demagnetised by reducing the magnetic field gradually to zero.

The system is capable of low-field measurements because the 24 bit resolution of the NI data acquisition card makes it capable of sensing signals as small as $10^{-6}$ V.

The secondary voltage was filtered to remove the dominant Faraday emf in order to obtain the BN signals. A digital band pass filter was used so that components in the range 25 kHz to 75 kHz were detected at a magnetizing frequency of 50 Hz. It was at this bandwidth that the Barkhausen emission which is maximum at the coercive points was detected. One search coil technique rather than a double coil arrangement was used to avoid losing some Barkhausen events in the subtraction process [10].

The major challenge in BN measurement is the reduction of background noise. The low noise NI4461 card with 24 bit resolution and a sampling rate of 204.8 KHz and 92 KHz bandwidth was chosen to take the measurements to minimize the influence of thermal noise. The card was placed in a PXI (**P**eripheral component interconnect e**X**tension for **I**nstrumentation) platform instead of in a computer system hence it operates in a predictable environment which means the measurements are more reliable and repeatable. In order to reduce environmental noise, the yokes, sample and search coil carrier were placed in a noise shielding chamber. Figure 3 shows the measurement system in the noise shielding chamber and the DAQ in a PXI interface. The computer monitor was remote from the measuring system to avoid interference with the measurements. Coaxial cables were used for all connection leads.

The acquired data was analysed using a number of algorithms that included root mean square (RMS) and total sum of amplitudes (TSA). The data was saved to a file for further processing after analysis.
RMS is the mean event amplitude over the range of flux in the BN cycle and is expressed as:

$$\text{rms}\,\psi = \sqrt{\frac{1}{N}\sum_{i=0}^{N-1} x_i^2} \quad (3)$$

where $x$ represents each event amplitude and N stands for the number of events.
The measured sum of amplitudes (over n cycles) is given by:

$$\text{Amplitude sum} = \sum_{i=1}^{Z=n} \left( \sum_{k=1}^{m} \left( \left| a_k \right| \right) \right)_i \qquad (4)$$

where variable ‘a’, represents the amplitude of a measured data point, index ‘k’ shows its position within the measured data point array ‘m’. Variable ’z’ indicates that the measurement has been taken n times successively. Index ‘i’ displays how often the measurement has been carried out [11].

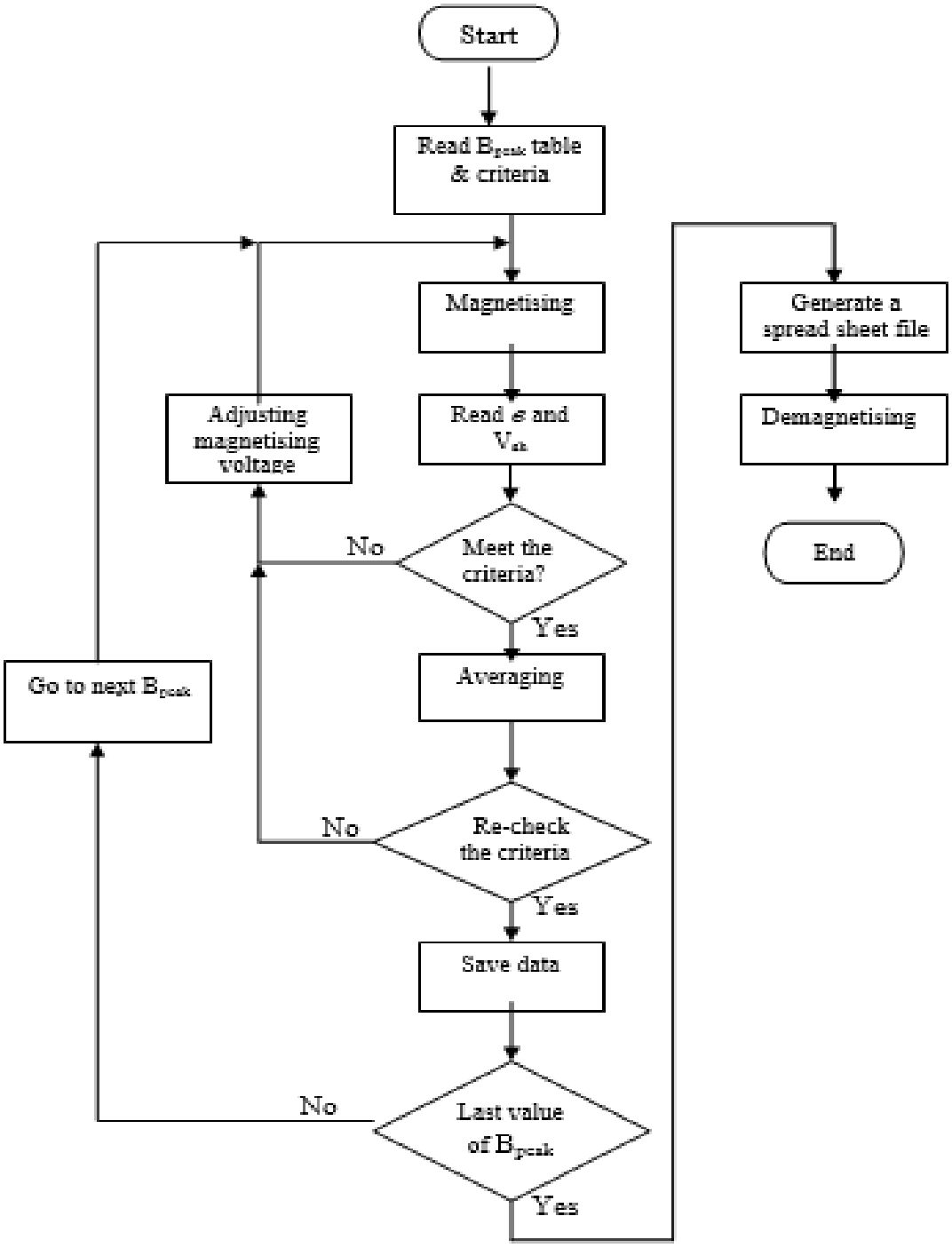


Fig. 2 Flowchart showing procedure of each measurement of the single strip tester

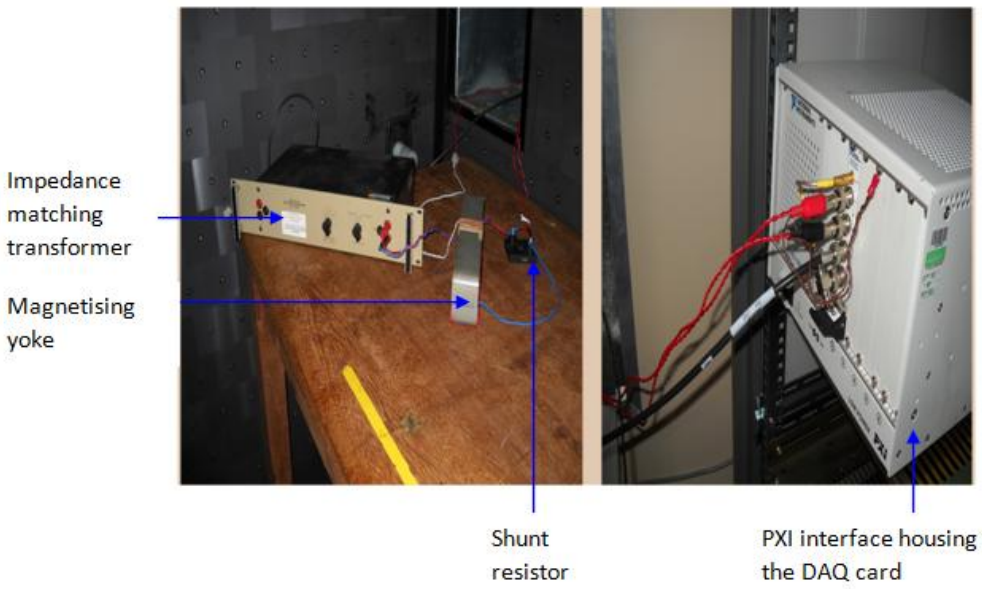


Fig. 3: Barkhausen Noise measurement system in the noise shielding chamber and the PXI platform housing the data acquisition card [12].

## III. RESULTS AND DISCUSSION

Figures 4 and 5 show typical BN spectra obtained from HGO and CGO steels at 1.2 T and 50 Hz. The sinusoidal curve is the flux density waveform at a 1000 times smaller scale. One cycle of magnetisation is shown. As expected, the BN is highest at points in time corresponding to when the material was experiencing maximum rate of change of magnetisation at the coercive fields [11, 13]. The coercive fields are the points where the flux density waveforms are zero in the figures. As can be observed from the figures, the BN amplitude is higher in HGO with the maximum peak occurring at 2mV while the maximum peak in CGO occurs at 1.4mV and this shows that the BN induced voltage in HGO is higher than that of CGO especially at high flux densities as subsequent results in this investigation show.

Figure 6 shows the RMS values of the BN spectra shown in figures 4 and 5 above as well as the background noise of the experimental set up at all the peak flux densities measured. Preliminary test determined the background noise level in the experimental set up. The same relationship was obtained when the background noise was plotted against the TSA. It can be observed from the figure that the background noise is more than 100 times less that the BN amplitude of the test samples. This was achieved by applying all the background noise reduction techniques outlined earlier. Background noise reduction is particularly challenging at very low inductions and measurements must be made in an environment free from electromagnetic interference.

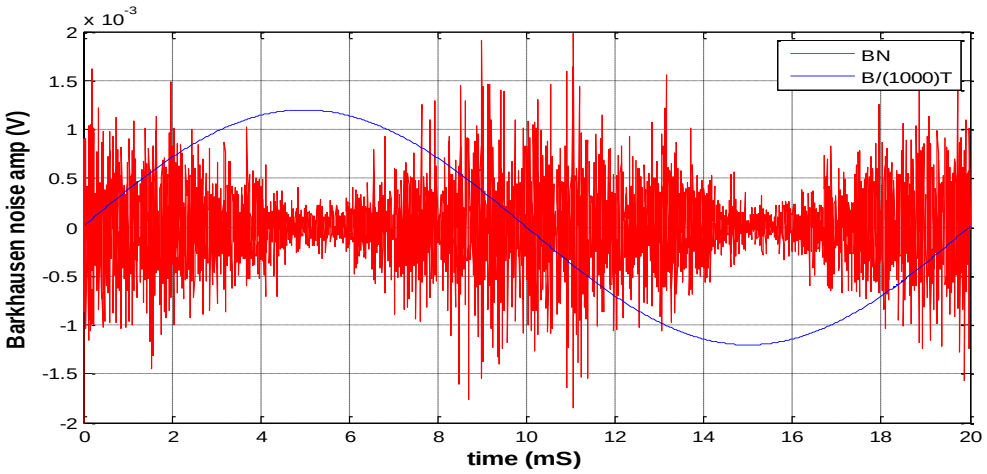


Fig.4: BN spectrum of HGO steel during one cycle of magnetisation at 1.2 T and 50 Hz showing variation of BN amplitude with time.

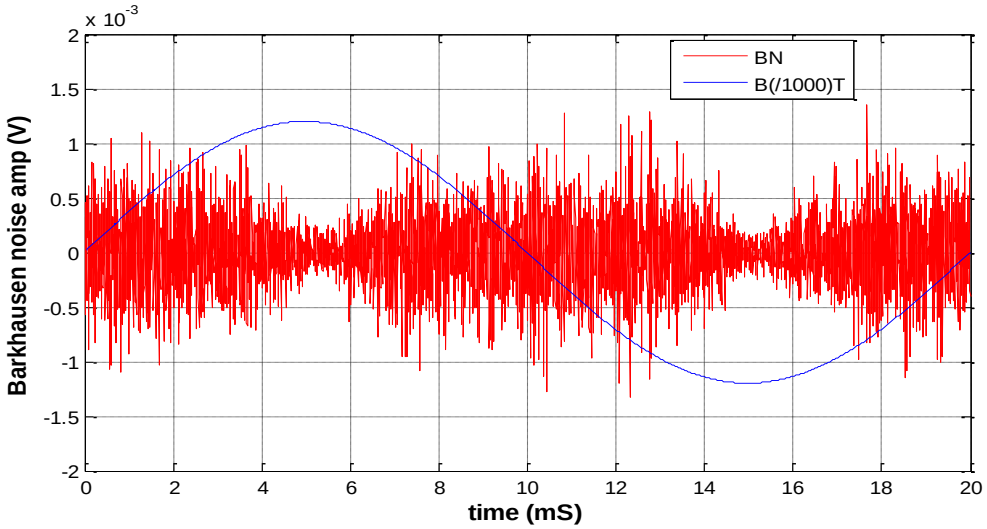


Fig. 5: BN spectrum of CGO steel during one cycle of magnetisation at 1.2 T and 50 Hz showing variation of BN amplitude with time.

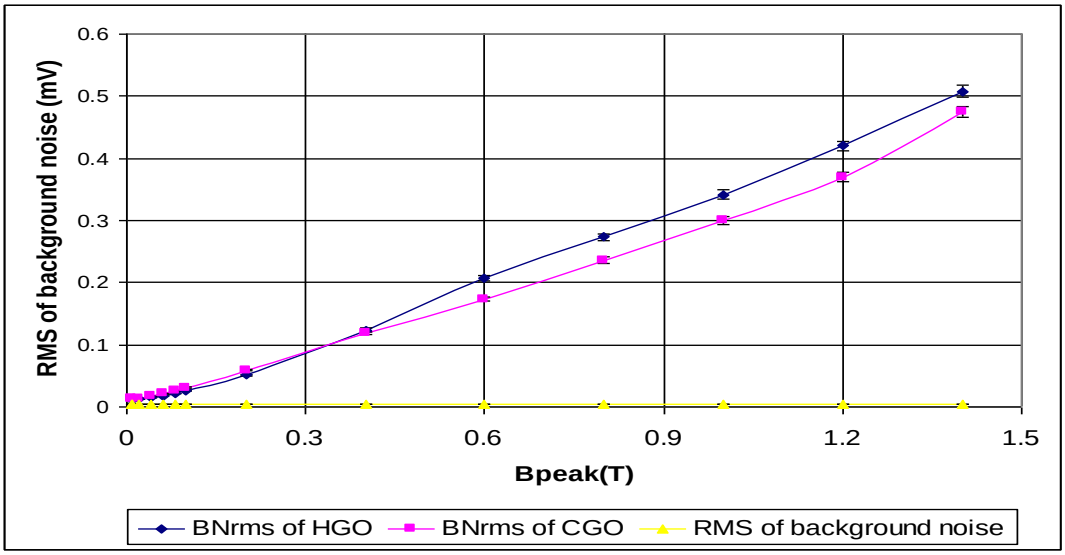


Fig. 6: Comparison of average rms BN of CGO and HGO strips at different flux densities at 50 Hz with background noise of Experimental set-up.

Figure 7 shows the variation of average RMS BN of 20 strips of CGO and 20 strips of HGO from P1 at both high and low flux densities. It can be observed that the average RMS BN is higher in HGO than in CGO above 0.2 T but at lower flux densities the trend changes. A similar characteristic was obtained when the same number of test samples from P2 was investigated at both magnetisation regimes. This is shown in figure 8. The variation of the percentage difference of the average rms BN of these test samples with peak flux density is shown in figure 9.

Figure 10 shows the same BN signals expressed in terms of the average TSA of BN peaks of the test samples from P1. As with the rms BN, the TSA of HGO is higher than that of CGO above 0.2 T and the trend changes at lower flux densities. TSA of samples from P2 show the same relationship as with P1 and is plotted in figure 11 with the variation in percentage difference at both high and low flux densities shown in figure 12.

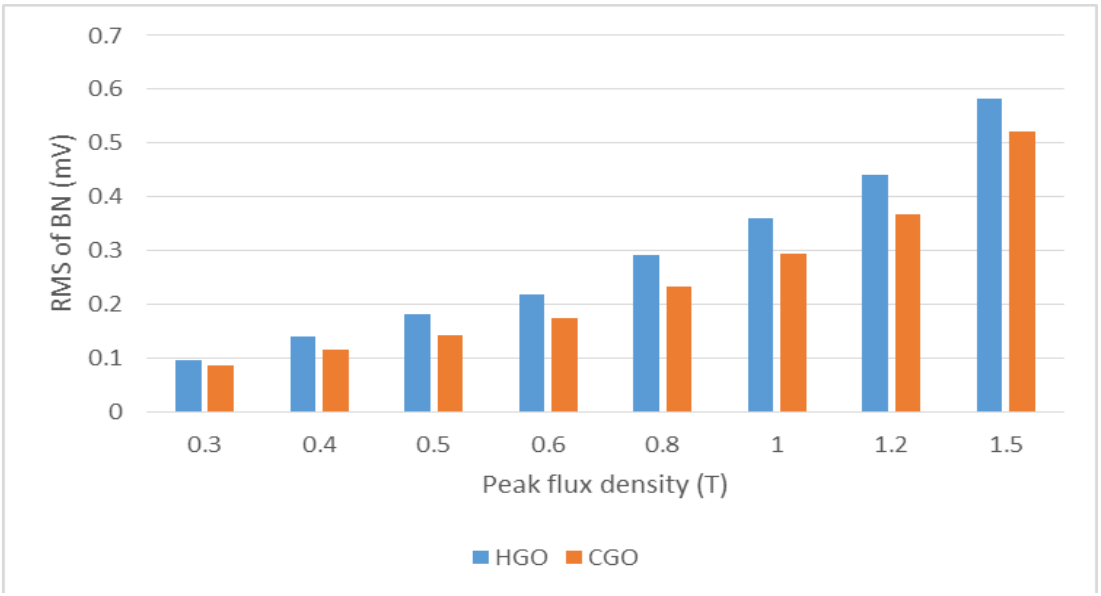


(a)

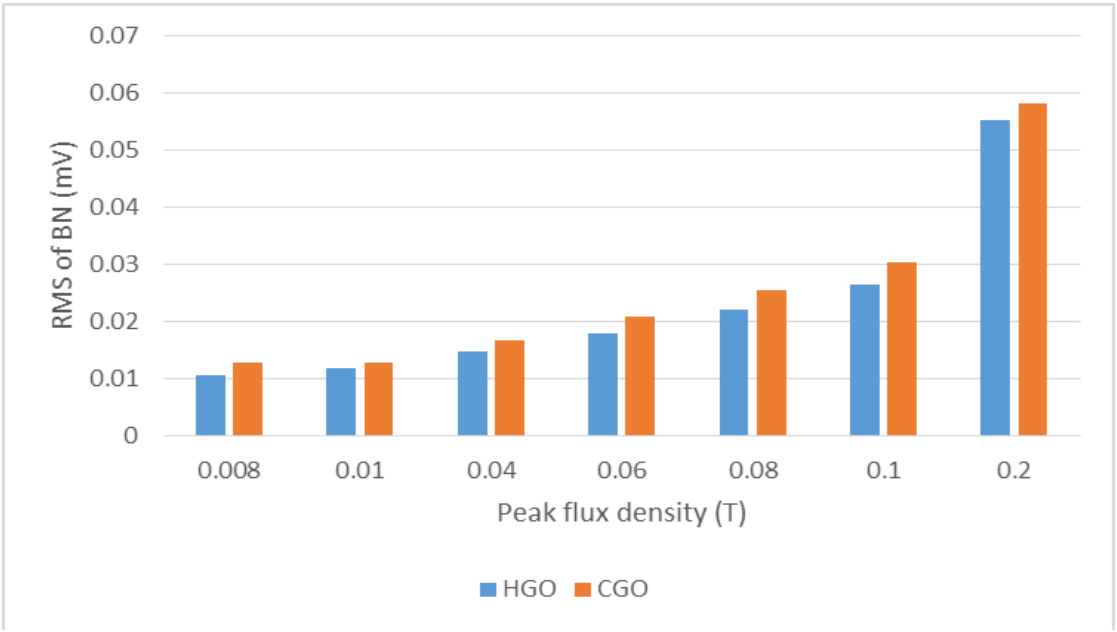


(b)

Fig. 7: (a) Variation of average rms BN of 20 strips each of CGO and HGO from P1 with peak flux density (b) the same comparison in the low field regime.

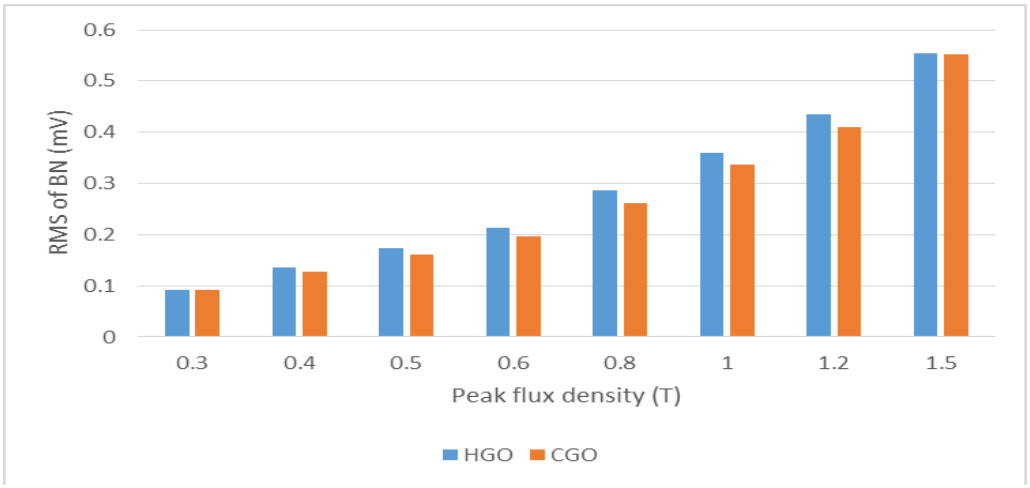


(a)

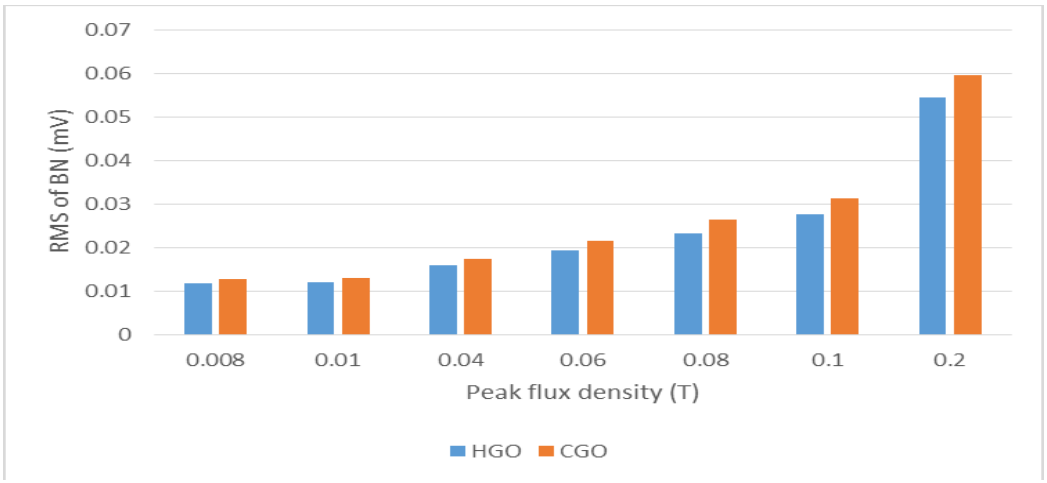


(b)

Fig. 8: (a) Variation of average BNrms of 20 strips each of CGO and HGO from P2 with peak flux density (b) the same comparison in the low field regime.

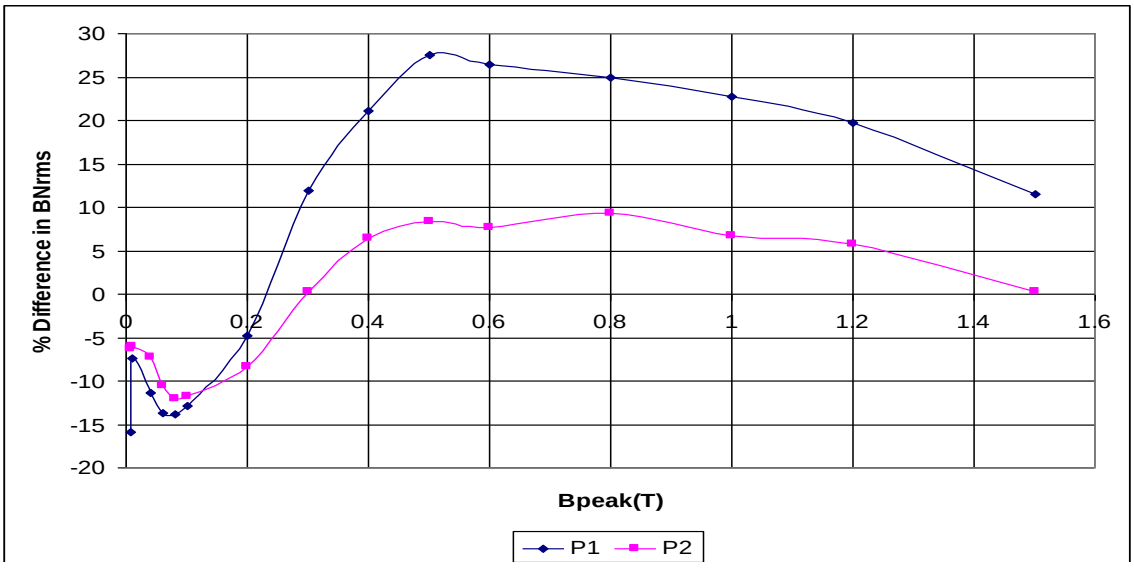


Fig. 9: Variation of percentage difference of average rms BN of HGO and CGO from P1 and P2 with peak flux density.

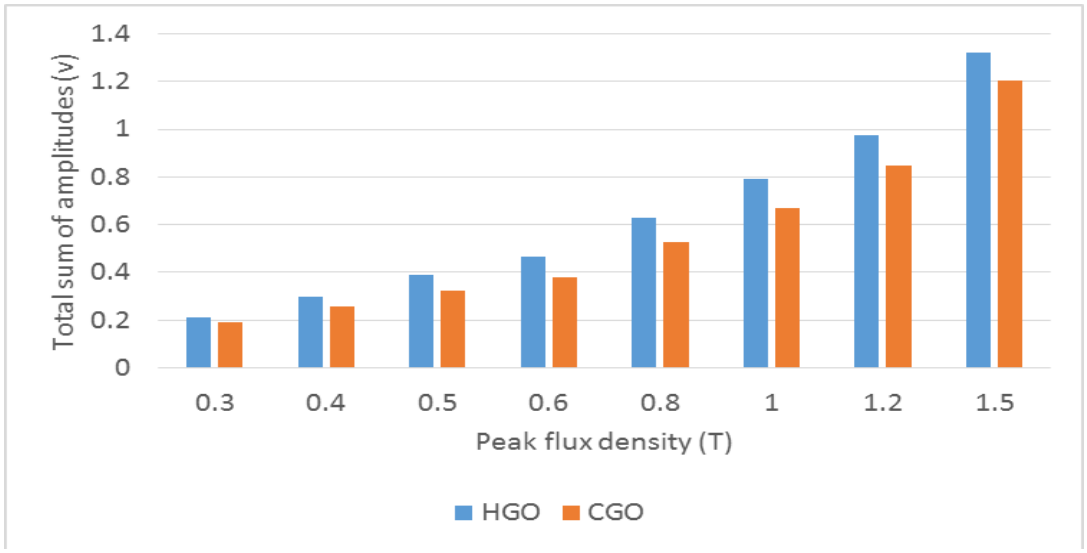


(a)

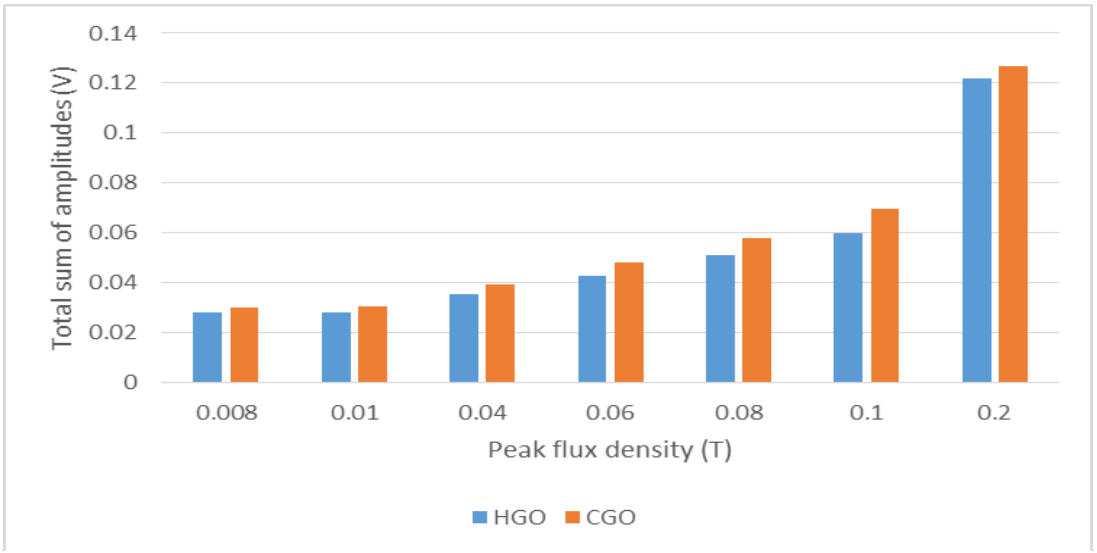


(b)

Fig. 10: (a) Variation of average TSA of 20 strips each of CGO and HGO from P1 with peak flux density (b) the same comparison in the low field regime.

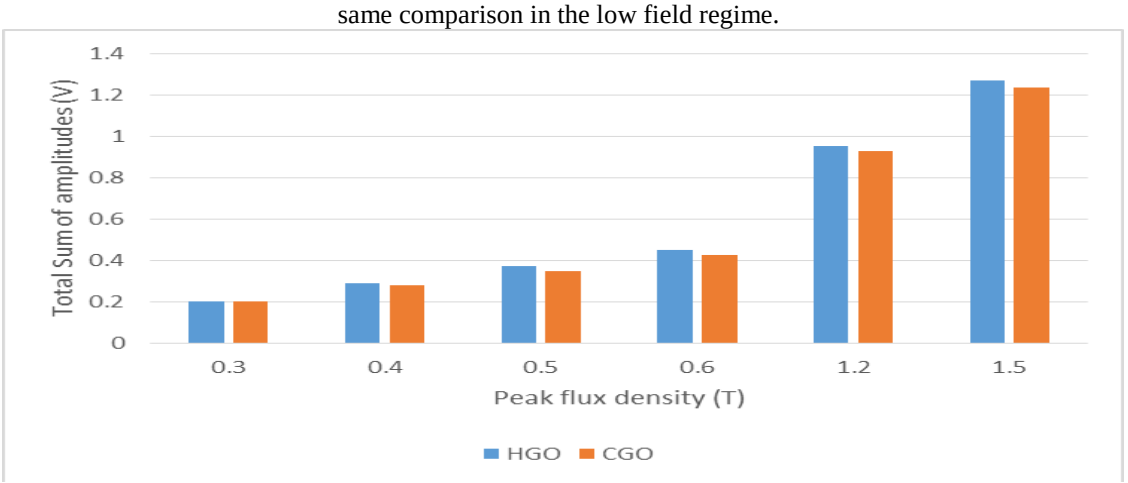


(a)

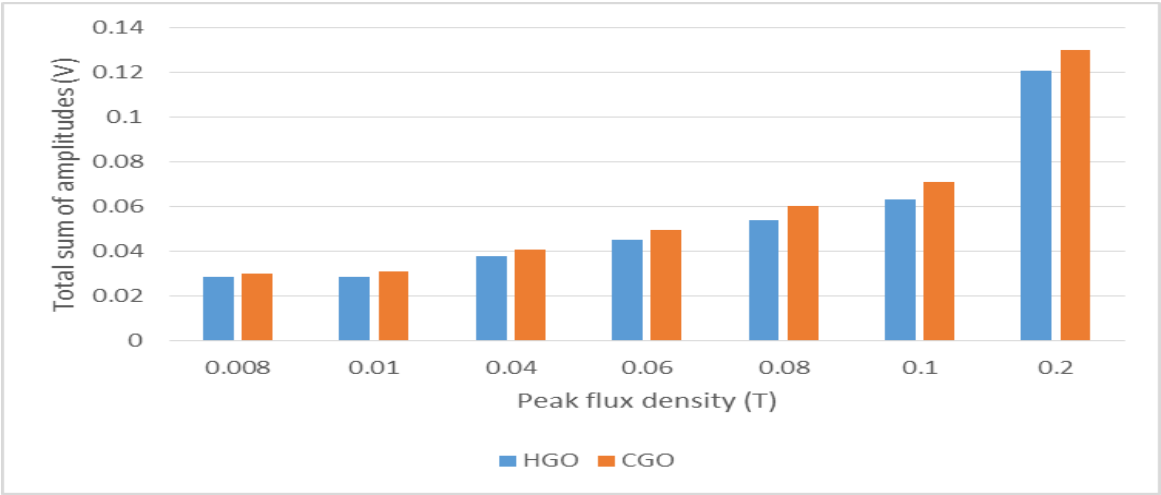


(b)

Fig. 11: (a) Variation of average TSA of 20 strips each of CGO and HGO from P2 with peak flux density (b) the same comparison in the low field regime.

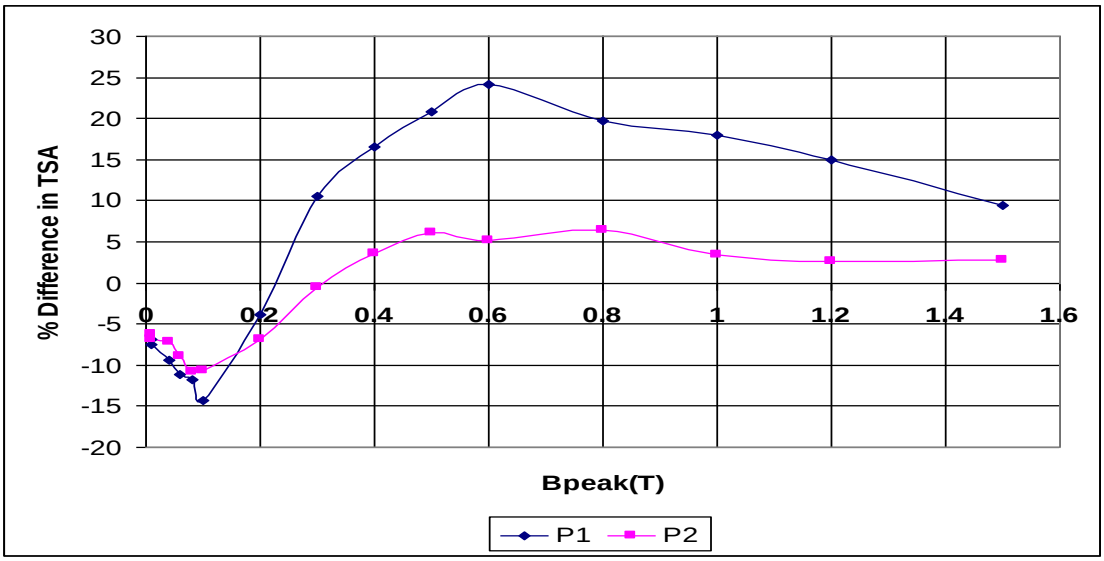


Fig. 12: Variation of percentage difference of average TSA of HGO and CGO from P2 with peak flux density.

As figures 9 and 12 show, it is interesting that below 0.2 T, the percentage difference in average rms BN of the test samples from P1 and P2 , and that of the average TSA respectively are very similar but at high flux densities, they are far different. This is because domain wall activity is higher at high flux densities so the effects of the difference in microstructure of the samples which account for BN will be more pronounced than at low field regime.

The observed higher BN response in terms of average rms and average TSA of HGO over CGO at higher flux densities in this work is because the grain size of HGO is higher than that of CGO and also grain to grain misorientation in CGO is higher than that of HGO. The domain width in GOES increases with increasing grain size. Increased grain size means that domain walls will move further between pinning sites and thereby generate larger changes in magnetization which results in a larger BN signal amplitude. The theoretical analysis below confirms that BN is proportional to the mean free path of domain wall movement.For the purpose of analysis of the theoretical relationship between BN and the microstructures of electrical steels, an induced voltage (Barkhausen) pulse is approximated by a Gaussian pulse to facilitate mathematical treatment [14].

A Gaussian pulse at a time t, is expressed mathematically as:

$$v(t) = \frac{A}{\sigma\sqrt{2\pi}} \exp[\ -(t - t_0)^2 / 2\sigma^2\ ] \qquad (5)$$

Where A is a quantity which is a function of maximum applied field, H, rate of change of field with time, dH/dt and the magnetic flux change, ΔΦ, in the magnetization region, σ is the pulse duration and $t_0$ is the time when the pulse is a maximum value. The total voltage induced in a search coil wound around a sample during experiment are obtained by summing the successive Gaussian pulses.
Assuming that σ and the time interval of Gaussian pulse, τ, are constant;

$$v_{total}\ (t) = \sum_{k=1}^{N} v_k\ (t) = \frac{A}{\sigma\sqrt{2\pi}} \sum_{k=1}^{N} \exp[\ -\{t - t_0 - (k-1)\tau\}^2 / 2\sigma^2\ ] \qquad (6)$$

where $v_k\ (t)$ the k'th Gaussian pulse and N is the number of total Gaussian pulses in a magnetization period, T.

$$N = T / \tau \qquad (7)$$

The amplitude value of the Gaussian pulse is

$$P_y = \frac{A}{\sigma\sqrt{2\pi}} \qquad (8)$$

The sum of the amplitude values of the Gaussian pulses, P, in a whole period, T, is

$$P = \int_T P_y\, dt \qquad (9)$$

The number of Gaussian pulses in T is N. The RMS value is the average of $P_y$ over the range of the time for magnetization reversal. Thus,

$$RMS = kP_y\tau = C_r \frac{\tau}{\sigma} \qquad (10)$$

where $C_r = \frac{AK}{\sqrt{2\pi}}$ depends on the magnetizing conditions and K is a constant. σ and τ are correlated with microstructure of the material and depends on the mean free distance.
When a domain wall moves from one pinning site to another, a Gauss pulse is generated and the Barkhausen jump occurs with a time duration σ.

$$\sigma = D / S \qquad (11)$$

Where D is the displacement of the domain wall (mean free distance) and S is the average speed of the domain wall movement.
The average speed of the domain motion is proportional to the external field, thus;

$$S = C_s H_n \qquad (12)$$

where $H_n$ is the minimum field strength of the external magnetic field required to unpin a domain wall from the pinning site and produce irreversible motion. $C_s$ is a proportionality constant.

$$H_n = \frac{1}{2\mu_0 M_s \cos\Theta} \left(\frac{\partial E}{\partial x}\right) \max \qquad (13)$$

where $\mu_0$ is the initial permeability, $M_S$ is the saturation magnetization, E is the domain wall energy, and Θ is the angle the external field axis makes with the direction of easy magnetization.

Assuming that the inclusion that pin a domain wall is spherical, its diameter is $l$ and its arrangement is a regular and simple cubic lattice, the domain wall is pinned and stopped in the center of the inclusion and the total free energy of the domain wall is a minimum. The wall is in the most stable condition.

Considering the area of a single domain wall in the inclusion lattice, suppose that the displacement of the domain wall is d after it is unpinned from an inclusion, the area of the domain wall:

$Y = b^2 - \pi(\frac{l^2}{4} - d^2)$ where b is the average grain diameter.

If q is the energy density of the domain wall, then the energy of the wall may be expressed as;

$$E_q = qY \quad (14)$$

when the domain wall moves a distance of d, the variation of the domain wall energy per volume is;

$\Delta E_q = \frac{\partial q}{\partial d} + \frac{q}{Y}\frac{\partial Y}{\partial d}$ , $q$ is a constant so;

$$\Delta E_q = \frac{q}{Y}\frac{\partial Y}{\partial d} = q\frac{\partial \ln Y}{\partial d} \quad (15)$$

Under the action of external field, H, when the domain wall is in the equilibrium state, $\Delta E_H + \Delta E_q = 0$

when the external field is varied, the energy of the $180^\circ$ domain wall will be:

$$-\Delta E_H = -\mu_0 M_s H \cos\Big|_{\Theta=0}^{\Theta=180} = \mu_0 M_s H \quad (16)$$

Substituting (15) into (13) and simplifying,

$$H_n = \frac{q}{2\mu_0 M_s H}(\frac{\partial}{\partial d}\ln Y) = \frac{\pi q l}{2\mu_0 M_s H b^2} \quad (17)$$

The volume swept by one domain wall, $V_w$, is approximated by a sphere:

$$V_w = \frac{4}{3}\pi\frac{l^3}{8} = \pi\frac{l^3}{6} \quad (18)$$

The ratio of the volume swept by a domain wall to the volume of a grain is expressed as;

$$\beta = \frac{\pi l^3}{6b^3} \quad (19)$$

Substituting (19) into (17),

$$H_n = (\frac{6}{\pi})^{\frac{1}{3}}\frac{k_1\delta}{\mu_0 M_s}\beta^{\frac{1}{3}}\frac{1}{b} \quad (20)$$

Where $\delta = \frac{q}{2k_1}$ which is the thickness of the domain wall and $k_1$ is the anisotropic coefficient of the material.

From (11) and (12),

$$\sigma = \frac{D}{C_s H_n} \quad (21)$$

Substituting (20) into (21);

$$\sigma = (\frac{\pi}{6})^{\frac{1}{3}}\frac{\mu_0 M_s}{C_s k_1 \delta}\beta^{\frac{1}{3}} D^2 \quad (22)$$

When the magnetization period, T, of the external field is constant and the time of producing a Barkhausen pulse is also constant, the total number of Barkhausen jumps in the magnetization process, N, is equal to the total number of pinning sites that caused domain walls to be pinned in the sweeping volume of the domain wall. The mean free distance of the domain wall is D, therefore,

$$N = \frac{1}{D^3} \quad (23)$$

From (7),

$$\tau = \frac{T}{N} = TD^3 \quad (24)$$

Substituting (22) and (24) into (10),

$$BNrms = C_f D \quad (25)$$

$C_f$ depends on the magnetization conditions.

This results of above analysis, (9) and (25), show that BNrms and amplitude sum is proportional to the mean free path of domain wall motion which is one of the bases of the interpretation of my experimental result.

Secondly, the grain-grain misorientation which is higher in CGO [15, 16] results in strong depression of the BN level which is caused by a decrease in the instantaneous rate of change of the magnetic flux during Barkhausen jumps, because of increased demagnetizing effects.

BN measurement has not been carried out at low flux densities (below 0.2 T) before. At low fields, domain wall motion has an intermittent, jerky character, with sparse Barkhausen jumps. The implication of this is that smaller grain samples (CGO) which have more grain boundaries acting as pinning sites and hence large fractional volume than HGO will have a greater number of these sparse Barkhausen jumps which will sum up to higher Barkhausen noise amplitude. This explains why at low flux density, the BN amplitude is higher in CGO material.

## IV. CONCLUSION

BN have been measured at power frequency at high and low flux densities and show repeatability for the discussed parameters. The use of low noise components was essential to obtain the signal.

The results presented show strong correlation between structure and BN in different grades of grain-oriented steel as well as interesting high and low field differences.This new understanding of low flux density performance of engineering magnetic materials will provide manufacturers with a more reliable and meaningful foundation for their designs thus leading to improved metering CTs and greater confidence of users in the accuracy of large scale electrical power measurement.

## REFERENCES


[1] J. P. Hall, Evaluation of residual stresses in electrical steel, PhD thesis, Cardiff University, 2001.

[2] A Moses, H. Patel, and P. I. Williams, AC Barkhausen noise in electrical steels: Influence of sensing technique on interpretation of measurements, Journal of Electrical Engineering, Vol. 57. No. 8/S, pp. 3-8, 2006.

[3] C. C. H. Lo, J. P. Jakubovics, and C. B. Scrub, Non-destructive evaluation of spheroidized steel using magnetoacoustic and Barkhausen emission, IEEE Transactions on Magnetics. Vol. 33, No. 5**,** pp.4035-4037, 1997.

[4] H. Kikuchi, K. Ara, Y. Kamada, and S Kobayashi, Effect of microstructure changes on Barkhausen noise properties and hysteresis loop in cold rolled low carbon steel, IEEE Transactions on Magnetics, Vol. 45, No.6 ,pp.2744-2747, 2009.

[5] M. F. de Campos, M. A. Campos, F. J. G. Landgraf and L. R. Padovese, Anisotropy study of grain oriented steels with magnetic Barkhausen noise, Journal of Physics, Conference Series 303, 012020, 2011.

[6] S. Turner, A. Moses, J. Hall and K. Jenkins, The effect of precipitate size on magnetic domain behaviour in grain-oriented electrical steels, Journal of Applied Physics, 107, 09A307-09A309-3, 2010.

[7] National Instruments, Dynamic signal acquisition user manual, August 2002.

[8] BS EN 10280:2001 + A1:2007, Magnetic Materials- Methods of measurement of the magnetic properties of electrical sheet and strip by means of a single sheet tester, British Standard, 2007.

[9] S. Zurek, P. Marketos, P. I. Anderson, and A. J Moses, Influence of digital resolution of measuring equipment on the accuracy of power loss measured in Epstein frame, Przeglad Elektrotechniczny (Electrical Reviews), Vol. R. 83, pp. 50-53, 2007.

[10] (www.omega.com/techref/pdf/strain-gage-technicaldata.pdf). Strain gauge technical data manufacturer's manual. Accessed on 15th July 2011.

[11] K. Hartmann, Relationships between Barkhausen noise, power loss and magnetostriction in grain-oriented silicon iron, PhD thesis, Cardiff University 2003.

[12] N. Chukwuchekwa, Investigation of Magnetic Properties and Barkhausen Noise of Electrical Steel, PhD thesis, Cardiff University, 2012

[13] H.V. Patel, S. Zurek, T. Meydan, D.C Jiles and L. LI, A new adaptive automated feedback system for Barkhausen signal measurement, Sensors and Actuators A, Vol. 129, pp.112-117, 2006.

[14] H Sakamoto, etal, IEEE Transactions on Magnetics, Vol. 23 No.5, Sept. 1987

[15] S. Taguchi, A. Sakakura and H. Takashima, US Patent 3287183, 1966.

[16] M. F. Littmann, Structures and magnetic properties of grain oriented 3.2% silicon-iron, Journal of Applied Physics, Vol. 38, issue 3, pp. 1104-1108, 1967.